

Particle Flow Control by Magnetically Induced Dynamics of Particle Interactions

F. Wittbracht*, A. Weddemann, A. Auge, and A. Hütten

Department of Physics, Thin Films and Physics of Nanostructures, Bielefeld University

*Universitätsstr. 25, 33615 Bielefeld, Germany, fwittbra@physik.uni-bielefeld.de

Abstract: In this work, we show that dipolar magnetic coupling can be used to control the particle flow through microfluidic structures without changing the state of motion of the carrier liquid. Also no external magnetic gradient fields are employed; the total external magnetic force applied is therefore zero. The theoretical idea will be tested experimentally. Here, additional effects originating from the interplay between hydrodynamic and electromagnetic interactions reveal that enhance the adaptability of the proposed method.

Keywords: self ordering, magnetic dipole interaction, particle flow control

1. Introduction

The integration of several tasks like injection, separation, purification or reaction of biological samples into a miniaturized microfluidic chip is a challenging task. Such *lab-on-a-chip* devices have attracted a lot of interest during the last decade due to many promising applications. Magnetic particles have revealed to be an important component since they can be manipulated by external magnetic fields originating from electromagnetic components on the size scale of the microfluidic geometry.^{1,2} Aligning their magnetic moment in field direction, they exert strong dipolar forces on each other if the particle concentration is sufficiently high. Especially, if high throughput is to be achieved these effects cannot be neglected anymore. Commonly such particle-particle interactions decrease the yield of the device since particles begin to agglomerate and form particle clusters which may behave in a different way.³ However, if their behaviour is predictable, this opens new strategies for the guidance and manipulation of magnetic markers in such devices.

We will introduce a method that though combining hydrodynamic and magnetic effects does not need electromagnetic structures on the

microscale. Thus, it is easy to implement and might decrease the complexity of existing microfluidic devices.

2. Governing equations

Magnetic particles dissolved in a carrier liquid move due to hydrodynamic as well as electromagnetic interactions. If we approximate each particle by a point mass, the motion of each individual particle can be calculated from Newton's second law

$$m \frac{dv}{dt} = \mathbf{F}_{\text{mag}} + \mathbf{F}_{\text{hyd}} \quad (1)$$

denoting by m the particle mass and by \mathbf{F}_{mag} and \mathbf{F}_{hyd} magnetic and hydrodynamic forces, respectively. However, especially on short distances electromagnetic interactions overcome fluidic contributions by far. If we assume a liquid velocity of $\mathbf{u} = 0$, we can restrict our model to magnetic interactions for right now. A magnetic moment $\mathbf{m}_{\text{part}}^1$ creates a magnetic field $\mathbf{H}_{\text{part}}^1$ at every space point \mathbf{r} that is given by the dipole expression (Fig. 1)

$$\mathbf{H}_{\text{part}}^1(\mathbf{r}) = \frac{1}{4\pi} \cdot \left(\frac{3\langle \mathbf{m}_{\text{part}}^1, \mathbf{r} \rangle \mathbf{r}}{|\mathbf{r}|^5} - \frac{\mathbf{m}_{\text{part}}^1}{|\mathbf{r}|^3} \right). \quad (2)$$

The stray field of the particle is inhomogeneous, thus, exerting a force $\mathbf{F}_{\text{mag}}^{21}$ onto a second magnetic particle / moment close by. If the susceptibility of the surrounding medium is omitted, this is given by

$$\mathbf{F}_{\text{mag}}^{21} = \mu_0 (\mathbf{m}_{\text{part}}^2 \cdot \nabla) \mathbf{H}_{\text{part}}^1. \quad (3)$$

with μ_0 the permeability of the vacuum.

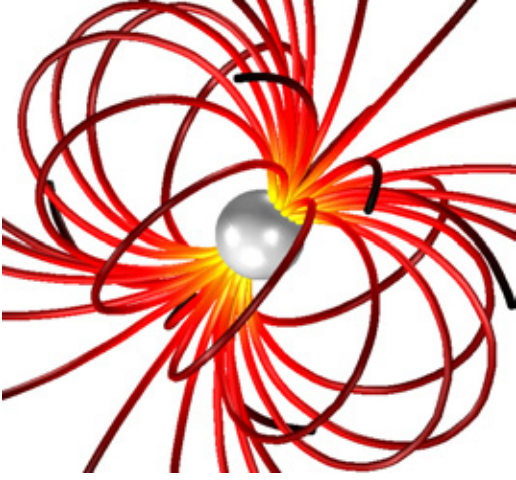


FIG. 1: Stray field of a magnetic single domain particle.

The direction of each individual magnetic moment depends on the total magnetic field. A magnetic moment \mathbf{m} in a field \mathbf{H} feels a torque

$$\boldsymbol{\tau} = \mu_0 \mathbf{m} \times \mathbf{H} . \quad (4)$$

favoring a parallel alignment of \mathbf{m} and \mathbf{H} . In principle all field contributions have to be taken

into account. However, we will restrict our analysis to the case of strong external fields validating the assumption of $\mathbf{m} \parallel \mathbf{H}_{\text{ex}}$. Since remagnetization processes occur on a nanosecond time scale, we can make the approximation of magnetic moment vectors that are perfectly aligned with the direction of the external field even for time dependent \mathbf{H}_{ex} .

A spatial particle distribution that is brought into a strong external magnetic field starts to assemble in rod like structures as shown in Fig. 2. Depending on the particle concentration chains of different particles numbers can be found. Changing the field direction leads to a rotation of the chains as long as the field frequency is not too high. The particle assemblies will rotate together with the field direction. Since particle-particle interactions along the chains are very strong, they can usually not be broken by fluid induced shear stresses. Therefore, chains can travel in microfluidic devices as confined objects.

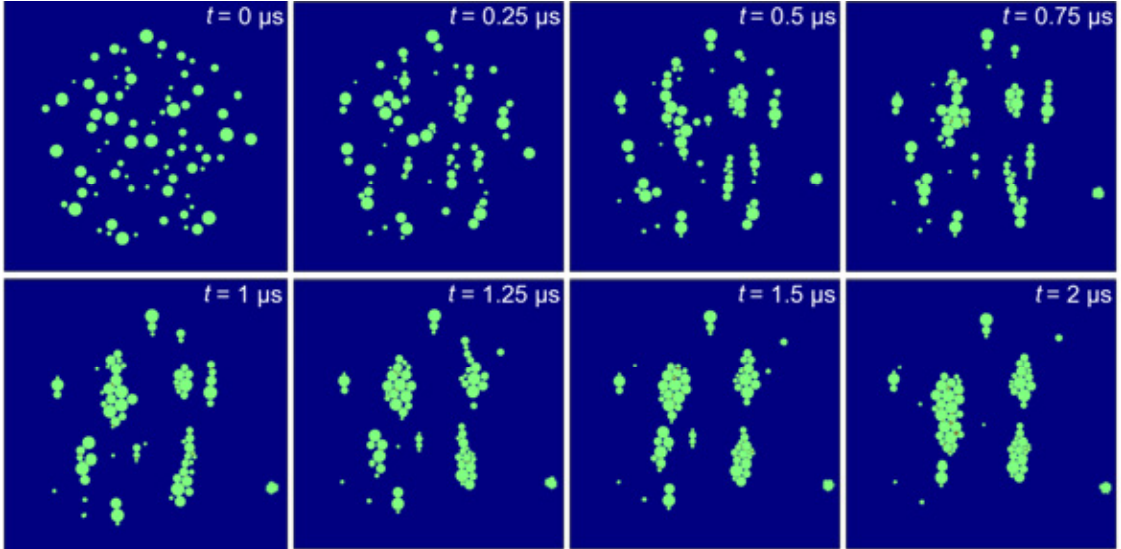


FIG. 2: Agglomeration of particles of sizes between 0.5 and 1 μm in homogenous magnetic field parallel to the y-axis. The saturation magnetization of the particles is set to 1000 kA/m, their initial configuration positions are chosen randomly on a two-dimensional sphere of radius 25 μm .

3. Model system

If magnetic chains as shown above are placed within a constant flow u they move very similar to pointlike objects. However, if inhomogeneous velocity fields are considered, an additional torque contribution exerts on the combined object. The orientation of the particle chain may differ from the field orientation. If the size scale on which the velocity changes is far bigger than the chain length L only small differences are noticeable. However, if they are on a similar size scale other effects can be found that can be used to control the motion of the chain. Such inhomogeneities can be introduced by the channel walls, a schematic of the main component is shown in Fig. 3. A circular reservoir is connected to a rectangular channel. The junction area may only be passed by particle chains of an orientation parallel to the flow direction in the channel. Perpendicular chains are blocked and remain within the reservoir or at the beginning of the junction. Creating chains by employing a homogenous external magnetic field, their alignment can be controlled by the field direction. Chains align parallel to the external field as long as changes are adiabatic, ensuring that the whole system is always at thermal equilibrium.

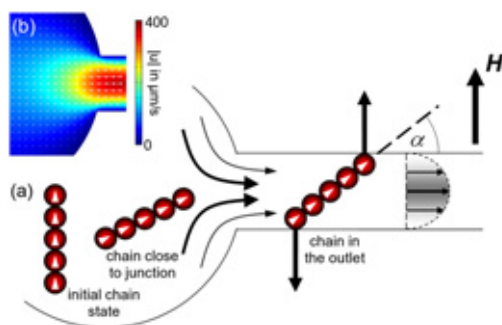


FIG. 3: Microfluidic reservoir-channel-junction. (a) A reservoir / reaction chamber is connected to a straight channel. Depending on the total torque acting on the chains, agglomerations get stuck at a certain position along the junction. (b) shows the velocity profile close to the junction.

4. Experimental realization and results

The microfluidic structures used in the experiments are built by optical lithography and soft lithography. The preparation of the microfluidic channels involves three lithography steps: 1) the design of the microfluidic geometry is structured onto a glass substrate using laser lithography and magnetron sputtering. The resulting partially metal coated glass substrate is used as a lithography mask in the second lithography step. 2) a negative of the channel geometry is realized on a siliconoxide terminated silicon wafer. In this process, the epoxy-based negative photoresist SU-8 3025 is spun onto the substrate and exposed to ultraviolet light through the lithography mask produced in the first step. The corresponding baking steps and exposure doses are chosen according to the manufacturers' instructions. The obtained SU-8 structure serves as a mold for the soft lithography step. 3) involves soft lithography using a polydimethylsiloxane (PDMS) polymer kit. The silicone elastomer is mixed with the curing agent in a mass ratio of 1:10. After mixing the polymer solution, the SU-8 structure is covered with a layer of the PDMS solution. The PDMS is cured at 80°C for 4.5 hours. After stripping the resulting PDMS channel geometry off the substrate it is trimmed with a scalpel and reservoirs are cut to enable inflow into the channels. The channels are sealed with a siliconoxide terminated silicon wafer. To ensure proper sealing of the microfluidic device, the silicon bottom plate and the PDMS channel geometry are treated with oxygen plasma leading to an irreversible sealing.

As already explained, to attain particle flow control, the characteristic length of the channel geometry needs to be comparable to the length of particle chains resulting from the self-ordering in a magnetic field. The investigated microfluidic device is shown in Fig. 4. The channels have a length of 2 mm, a height of 25 μm and a width of 30 μm . The reservoirs have a radius of 500 μm . In order to ensure sufficient percolation of the carrier liquid along the reaction site an elliptically shaped reaction chamber is chosen. The lengths of the short and the long semiaxis of 160 and 90 μm , respectively. The experimental setup consists of a pair of coils for the generation of an in-plane homogeneous magnetic field. The field strength can be adjusted up to 490 Oe. The

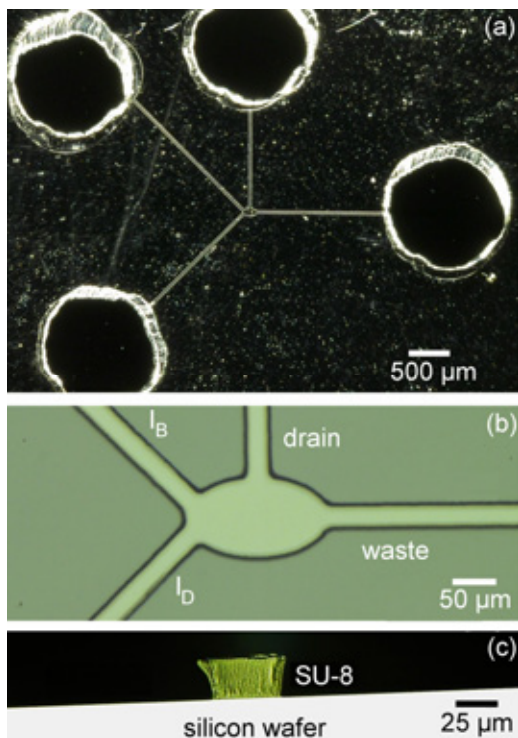


FIG. 4: Optical microscopy images of the microfluidic device. (a) shows an overview of the channel geometry, (b) microfluidic channels of $30\ \mu\text{m}$ width end in the reaction chamber of elliptical shape. (c) A cross-section image of the SU-8 mold leading to the estimation of a channel height of $25\ \mu\text{m}$.

microfluidic device is positioned on a pivotable sample holder in the center of the coil arrangement. The experiments are recorded with a digital optical microscope and with a built-in charge-coupled device (CCD) camera enabling to record up to 28 frames per second. Due to the agglomeration of particles as discussed above, superparamagnetic beads are used in the experiments in order to enable dissolving of bead clusters, when the magnetic field is switched off. To distinguish beads flowing from the different reservoirs, magnetic markers with different sizes and narrow size distributions are necessary. Dynabeads MyOne™ ($d = 1.05\ \mu\text{m}$) and M-280 ($d = 2.8\ \mu\text{m}$) are used in the experiments.⁴ These beads fulfill the requirements mentioned above: they are superparamagnetic and have size distributions with standard deviations lower than 2%. Both bead solutions have a concentration of $c = 10\text{mg/ml}$.

At the beginning of the experiment a magnetic field of 490 Oe is applied and a $1\ \mu\text{l}$ droplet of de-ionized water is inserted into the drain leading to a filling of the microfluidic device in order to eliminate wetting effects. The bead reservoirs I_B and I_D are filled with MyOne™ and M-280 bead solutions. While the bead solutions are applied, the magnetic field vector is parallel to the drain channel direction. Due to chain formation in the reservoirs I_B and I_D , no particle flow can be observed as long as the magnetic field orientation is not changed.

Rotating the sample towards a parallel alignment of magnetic field and the channel leading to reservoir I_D enables flow of particle chains from I_D to the reaction chamber as presented in Fig. 5(a). The particle chains consist of Dynabeads M-280 only and no flow of Dynabeads MyOne™ can be observed. The flow of M-280 beads can be inhibited by sample rotation into another direction. The alignment of the magnetic field in direction B enables flow of

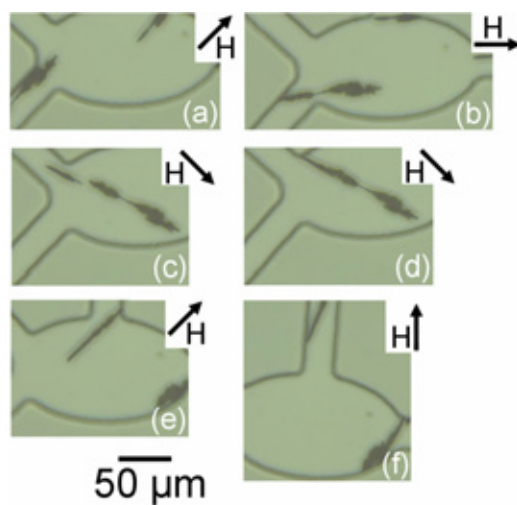


FIG. 5: Microscopy images of the microfluidic device during operation. (a-b) A bead chain consisting of Dynabeads M-280 enters the reaction chamber from the inlet channel I_D . (c) Switching to another field orientation leads to flow of MyOne™ bead chains from the inlet I_B to the reaction chamber. (d) After both bead chains reach the reaction chamber, a larger agglomerate consisting of two bead species is formed. (e-f) The reaction chamber can be emptied through the drain channel by changing the orientation of the magnetic field and the microfluidic system. The image series covers a time step of 8.5 s.

MyOne™ bead chains to the reservoir as shown in Fig. 5(c). For both orientations B and D, particle flow through the drain channel is blocked. After entering the reaction chamber, the MyOne™ bead chain merges with the residual M-280 chain to form a larger agglomerate consisting of two bead species (Fig. 5(d)). Aligning the magnetic field with the drain channel washes the bead chain out of the reaction chamber as shown in Fig. 5(f).

An additional self ordering effect can be observed visualizing the interplay of magnetic and hydrodynamic forces. In Fig. 6 a bead chain consisting of Dynabeads M-280 is shown. The chain aligns with the magnetic field and hits the channel wall while traveling through the reaction chamber as presented in Fig. 6(a). The interaction of the bead chain with the carrier liquid leads to a rotation along the long semiaxis of the chain. The single rotation steps can be seen in Fig. 6(b).

Conclusion

Particle-particle interactions can be used for particle flow guidance in microfluidic devices. The proposed setup operates without any electromagnetic components on the microscale but is completely controllable by a homogenous macroscopic magnetic field. Therefore, this method may help to strongly reduce the complexity of existing and future lab-on-a-chip systems.

Literature

- ¹A. Weddemann, F. Wittbracht, A. Auge, A. Hütten, *Appl. Phys. Lett.* **94**, 173501 (2009)
- ²A. Auge, A. Weddemann, F. Wittbracht, A. Hütten, *Appl. Phys. Lett.* **94**, 183507 (2009)
- ³A. Weddemann, A. Auge, F. Wittbracht, S. Herth, A. Hütten, *Proc. Europ. COMSOL Conf. Hannover 2008*, ISBN 978-0-9766792-8-8
- ⁴G. Fønnum, C. Johannson, A. Molteberg, S. Mørup, and E. Aksnes, *J. Magn. Magn. Mater.* **293**, 41 (2005)

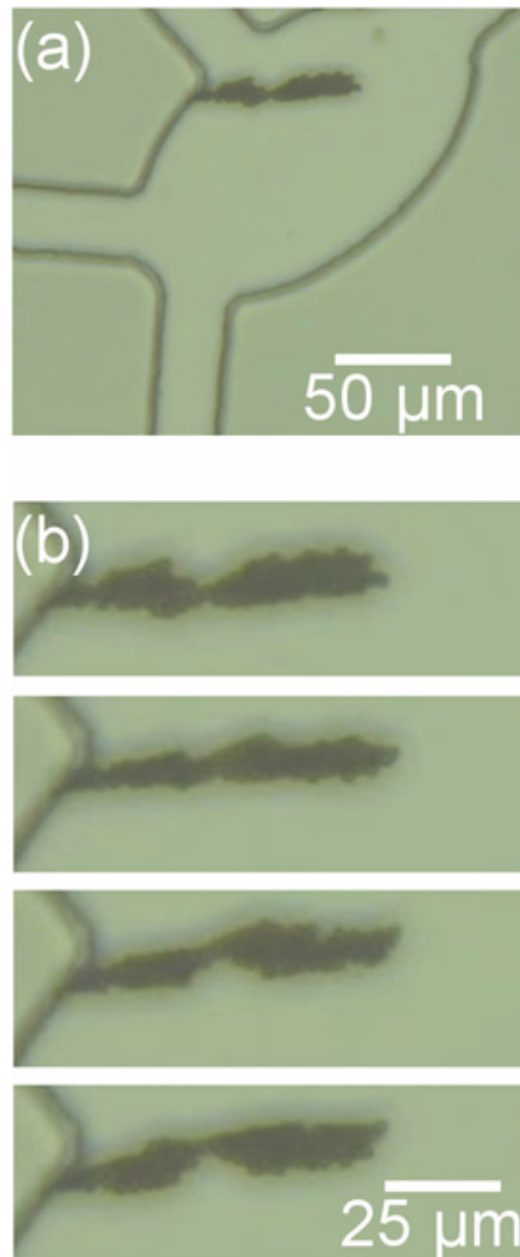


FIG. 6: Microscopy image of an additional effect occurring in the microfluidic device. (a) A bead chain consisting of Dynabeads M-280 aligns with the magnetic field and hits the reaction chamber wall. (b) According to interaction of fluidic and magnetic phenomena, the bead chain rotates along the long semiaxis (b).